iJRASET
International Journal For Research in Applied Science and Engineering Technology



INTERNATIONAL JOURNAL FOR RESEARCH

IN APPLIED SCIENCE & ENGINEERING TECHNOLOGY

Volume: 11 **Issue:** IV **Month of publication:** April 2023

DOI: https://doi.org/10.22214/ijraset.2023.51877

www.ijraset.com

Call: 08813907089 | E-mail ID: ijraset@gmail.com

International Journal for Research in Applied Science & Engineering Technology (IJRASET)
ISSN: 2321-9653; IC Value: 45.98; SJ Impact Factor: 7.538
Volume 11 Issue IV Apr 2023- Available at www.ijraset.com

Grid Sychronization of Wind Based Microgrid

Dr. G. V. Naga Lakshmi[1], A. Srinika[2]
[1, 2]*Department of Electrical Engineering, University College of Engineering (A) Osmania University, Hyderabad - 500 007, Telangana State, India*

Abstract: ***This paper presents the methods for synchronization of a wind based micro grid with main grid. The wind power is generated using the permanent magnet brushless DC generator (PMBLDCG) and the MPPT (Maximum Power Point Tracking) is executed with P&O (Perturb & Observe) approach to extract the maximum power from the wind generation. This power is fed to the AC load using a voltage source inverter (VSI) through the battery bank (BSS) at DC link. The control algorithm operates in standalone mode and grid connected mode. It can switch between islanded and grid connected modes seamlessly according to the wind conditions. In standalone mode, this wind power is fed to the load through a VSI, during low wind conditions; the battery discharges itself to fulfill the load demand. After that, the grid is connected to give power to the load during low wind conditions, and for this, control algorithm operates in grid connected mode. Therefore, the control algorithm switches from voltage control to current control mode to provide smooth synchronization and vice versa at de-synchronization. A MATLAB Simulink model is developed to simulate the system performance during wind variations and load, and during synchronization and de-synchronization.***

Keywords: Wind turbine, Permanent Magnet Brushless DC Generator, Micro Grid, Main Grid.

I. INTRODUCTION

Modern advanced civilization is standing on the feet of electrical energy. This energy is generated mainly from the conventional resources based on fossil fuels. However, in this world of technical advancement and development only conventional energy resources are not sufficient. Therefore, renewable resources have also been explored and research on these fields is also getting maturity [1]. The local demand of energy is fulfilled with distributed energy generation, and micro grid is one of such ways that consists of resources like wind, solar, hydro, and biogas etc. These sources increase energy efficiency, reduce losses; enhance the robustness of such sources [2]. They can also feed the extra power to the utility grid through power electronics converters. Therefore, the converters of these micro grid systems have to work in both standalone and grid connected modes. Various control algorithms for standalone system have been used in previous literature to improve the power quality, stability and performance of such systems. The control algorithms of grid connected system are also defined. These control algorithms generate the PWM pulses for the switching of the converter according to the operating mode. These converters are being used for smooth transition between grid connected and standalone modes to transfer the energy coming from the distributed generation or microgrids. It must be transients free during transfer. These control algorithms are based on voltage control and current control approach. In literature, a thorough control description is given on grid connected, standalone and rectifier modes for multifunctional PWM converter. It is given with the PLL (Phase Lock Loop) approach to extract grid angle[3]. An indirect current control method is used for seamless transfer of distributed generation system for intentional islanding. It is also provided with LC filter design. In previous models, a control strategy is explained with single control structure including both the modes of operation and smooth transition without PLL approach.

In this work, the control algorithm switches in two modes in voltage and current control modes according to the availability of wind. The microgrid works in standalone mode when sufficient wind power is available and excess power is stored in battery during high winds. When wind generation is small and demand is increased the battery starts exhausting and if the grid is available the synchronization process takes place seamlessly [4]. Now the converter starts operating in current control mode from the voltage control mode. Here SOGI (Second Order Generalized Integrator) based PLL (Phase Lock Loop) is used to extract the grid angle. The wind energy conversion system (WECS) includes wind turbines, generators, control system, interconnection apparatus. Wind Turbines are mainly classified into horizontal axis wind turbines (HAWT) and vertical axis wind turbines (VAWT). Modern wind turbines use HAWT with two or three blades and operate either downwind or upwind configuration. This HAWT can be designed for a constant speed application or for the variable speed operation [5]. Among these two types variable speed wind turbine has high efficiency with reduced mechanical stress and less noise.

©IJRASET: All Rights are Reserved

Variable speed turbines produce more power than constant speed type, comparatively, but it needs sophisticated power converters, control equipments to provide fixed frequency and constant power factor.

II. WIND POWER- STATISTICS

Wind power is one of the fastest-growing renewable energy technologies. Usage is on the rise worldwide, in part because costs are falling. Global installed wind-generation capacity onshore and offshore has increased by a factor of almost 75 in the past two decades, jumping from 7.5 gigawatts (GW) in 1997 to some 564 GW by 2018, according to IRENA's latest data. Production of wind electricity doubled between 2009 and 2013, and in 2016 wind energy accounted for 16% of the electricity generated by renewables. Many parts of the world have strong wind speeds, but the best locations for generating wind power are sometimes remote ones. Offshore wind power offers tremendous potential. Wind turbines first emerged more than a century ago. Following the invention of the electric generator in the 1830s, engineers started attempting to harness wind energy to produce electricity. Wind power generation took place in the United Kingdom and the United States in 1887 and 1888, but modern wind power is considered to have been first developed in Denmark, where horizontal-axis wind turbines were built in 1891 and a 22.8- metre wind turbine began operation in 1897.Wind-turbine capacity has increased over time. In 1985, typical turbines had a rated capacity of 0.05 megawatts (MW) and a rotor diameter of 15 metres. Today's new wind power projects have turbine capacities of about 2 MW onshore and 3–5 MW offshore. Commercially available wind turbines have reached 8 MW capacity, with rotor diameters of up to 164 metres. The average capacity of wind turbines increased from 1.6 MW in 2009 to 2 MW in 2014.Wind is the second most widely used renewable energy source, as global installed wind capacity exceeded 591GW in 2019, accounting approximately 25% of the total renewable energy generation capacity. In India, as of November 30 2020, total installed capacity of renewable energy is 136GW, out of which 38.42GW is wind power that means wind power accounts to 42% of the Indian renewable energy [6].

III. CONTROL SYSTEM

The control of the inverter needs to change according to the various operating modes. In standalone mode it operates in voltage control mode and in grid operating condition it works in current control mode. During synchronization and de-synchronization process this control algorithm has ability to switch between both the modes [7]. This swift between two control algorithms must be very smooth to avoid grid current and voltage transients.

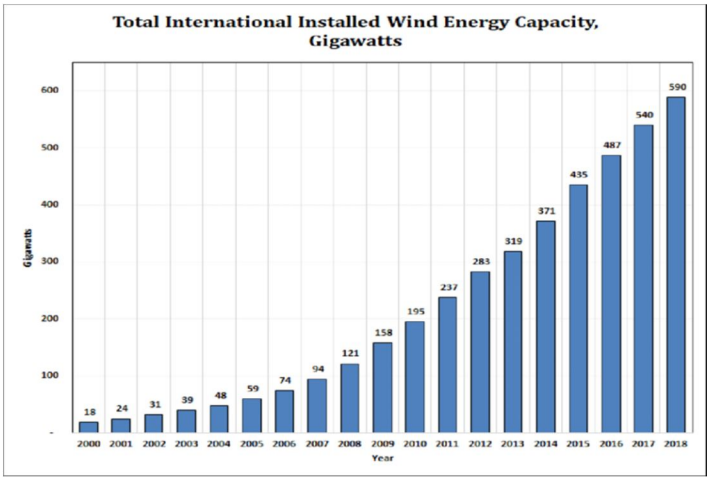


Figure. 1. Total Installed Wind Capacity in GW

A. *Control for Standalone Mode of Operation*

In standalone mode of operation, the microgrid VSI PWM pulses are generated from voltage control algorithm. The reference sine voltage is generated with reference voltage magnitude and frequency (V*, wo) and is compared with feedback voltage to generate PWM pulses for voltage source inverter.

In this mode of operation, wind power is rectified by a three phase diode bridge rectifier, whose output is given to a boost converter and there exists a battery storage system which can be charged when the wind speed is higher than the power required by the load and also in case of lower wind speeds the mechanical output power of the wind turbine will not be able to meet the load in such a case the pre charged battery can be can feed the load [8].

B. Control for Grid Connected Mode of Operation

In grid connected operation the control algorithm works on indirect current control algorithm with power factor correction (PFC) mode as shown in Fig.3. The fundamental load current component for phase 'a' (iLf) is extracted using SOGI (Second Order Generalized Integrator) filter as shown in Fig.4. This is used to estimate active power component (ILp). To keep ILf in phase with its respective voltage, quadrature template (uq) is given as input to a zero crossing detector (ZCD). The in-phase (up) and quadrature (uq) components of the grid voltage are derived according to Fig.6. The current signal iL is input signal for sample and hold circuit (SHC) and triggering pulse comes from output of ZCD[9]. The active power component of the iLa is extracted as an output. The reference current component is derived as, i_g^*=i_Lp u_p. The reference grid current (i*g) and sensed grid current (ig) are compared to generate PWM pulses for the switching of VSC in grid connected mode.

C. Transition From Standalone to Grid Synchronization

For the smooth transition from standalone to grid connected mode, the load voltage magnitude, frequency and phase must be within the range according to IEEE 1547 standard. Once these parameters match the microgrid is connected to the utility grid through STS [10]. The steps of synchronization are explained as:

1) When the grid is present in normal operating condition.
2) Check the voltage magnitudes at PCC and grid. If the difference is less than 10% according to IEEE 1547 standards upto 500 kVA in distributed generation.
3) Calculate the in-phase (up) and quadrature (uq) template of grid voltage and load voltage using SOGI as shown in Fig.5. Match up with load voltage in-phase template as shown in Fig.6. For smooth synchronization the angle difference sin (8g- 8SA) = (8g- 8SA) = a, is taken less than 2°, which is within the limits provided by the IEEE standard 1547.
4) Now a signal is generated to switch on the STS for grid synchronization of microgrid. Simultaneously, the control mode switches form the voltage control mode to current control mode.

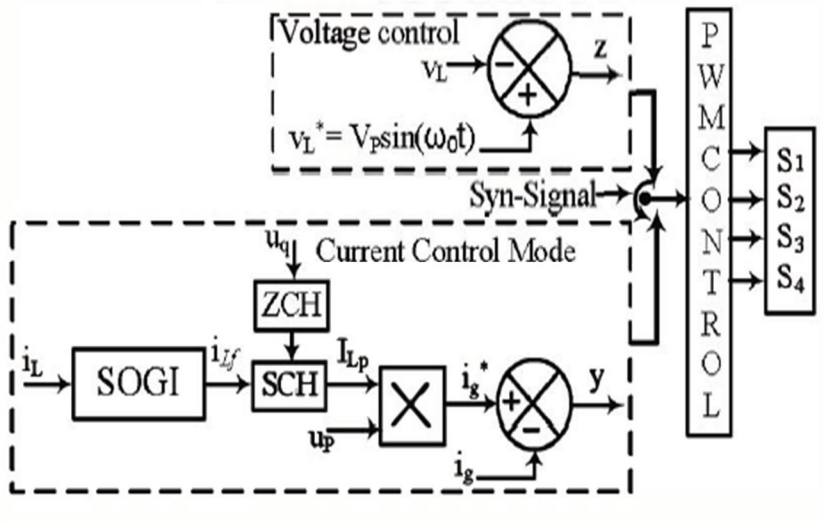


Fig. 2. Voltage and Current Control for Grid Connected Operation

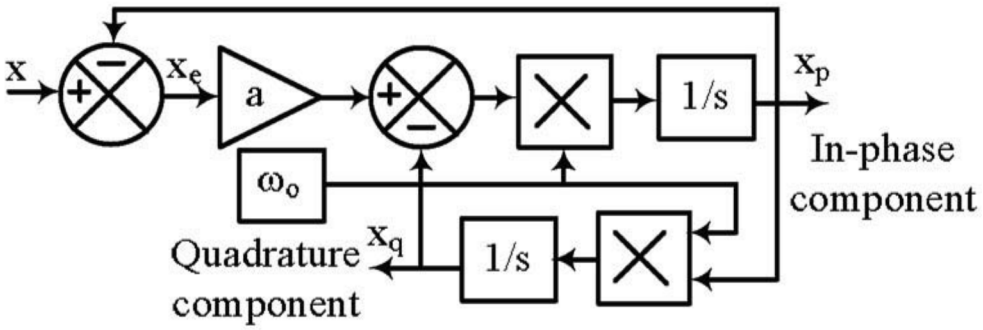


Fig. 3. SOGI (Second Order Generalized Integrator)

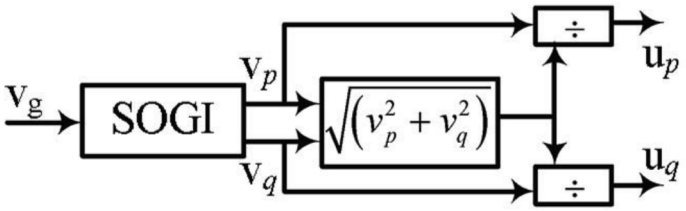


Fig. 4. In-phase and Quadrature Components of Grid Voltage

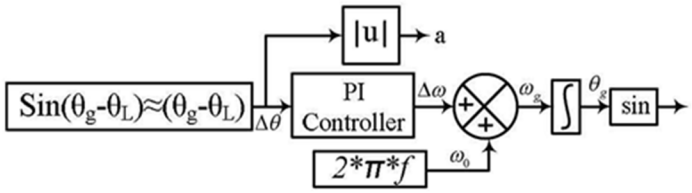


Fig. 5. Phase Angle Matching using PI Controller

D. Transition From Grid Synchronization to Standalone Operation

When the grid is not available or wind power is sufficient to supply load demand. The microgrid appears back to standalone mode of operation. The necessary steps for de-synchronization are explained as,

1) The grid is unavailable.
2) At this time the voltage difference between PCC and grid voltage becomes large.
3) De-synchronization signal is produced.
4) The control mode changes to voltage control mode and simultaneously the STS switches off
5) To avoid sudden jump of the angle, the initial value of the angle at the instant of control mode change is kept same as that of during synchronization.

E. Phase Locked Loop

In grid connected applications the synchronization of output signals of the converters to be connected with grid parameters-frequency and phase is of great importance. Different methods based on Fourier transforms, zero-crossing detection, Kalman filters, phase-locked loops (PLL) and others are used for this synchronization [11].

Among all these methods PLL is one of the popular methods used in grid connected systems because of the simple implementation and robustness under different grid conditions. A PLL is a device providing tracking of one signal by another one and as a result of this tracking the output signal is synchronized with the input reference signal in phase and frequency. The classical PLL consists of three general blocks – i) Phase Detector ii) Loop Filter (LF) iii) Voltage Controlled Oscillator (VCO).

Classification and explanation of the basic operation of the most commonly used types of control and synchronization are presented in [12]. Increasingly in the literature one can find separate approaches in the implementation of the PLL in three-phase and single-phase applications. In grid connected three-phase applications the synchronous-reference frame is very commonly used. The main idea of the synchronous-reference frame PLL is the transformation of the input signals in dq-frame by means of the well-known Park and Clark transformations [5]. In case of operation of the grid-inverter in polluted utility grid to improve the quality of the energy an adaptive synchronous reference frame PLL is used.

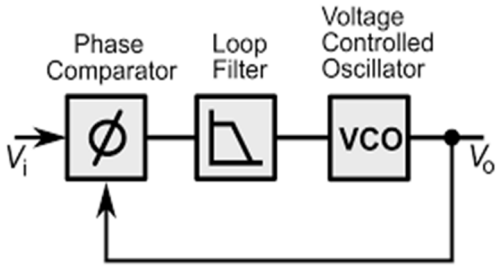


Fig. 6. Block diagram of a single-phase PLL

The Park-PLL and SOGI-PLL are two widely used single-phase PLLs that are immune to the change of the grid frequency, and have certain filtering ability. The SOGI-PLL uses two first-order integrator to construct the OSG based on second-order generalized integrator, which is easy to be implemented digitally, and the nonlinearity is lower than that of Park-PLL [13].

The structure of SOGI-PLL is shown in Fig. 4, in which ug is the input signal, ωff (=2π50 rad/s) is the central angular frequency, ωPLL and θPLL are the estimated angular frequency and phase angle, respectively [6]. It can be seen from Fig. 4 that the SOGI generates a pair of orthogonal signals (i.e., uα and uβ), which are then sent to the Park transformation module (i.e., αβ →dq) to obtain ud and uq

$$\begin{bmatrix} ud \\ uq \end{bmatrix} = \begin{bmatrix} cos\theta PLL & sin\theta PLL \\ -sin\theta PLL & cos\theta PLL \end{bmatrix} \cdot \begin{bmatrix} u\alpha \\ u\beta \end{bmatrix} \text{.....(1)}$$

Assuming that the input signal is a pure sinusoidal in the form of ug = Vm cos θg, and that the SOGI outputs a pair of signals with the same amplitude as the input signal and a phase difference of 90◦ , (1) can then be rewritten as

$$\begin{bmatrix} ud \\ uq \end{bmatrix} = \begin{bmatrix} Vmcos(\theta g - \theta PLL) \\ Vmsin(\theta g - \theta PLL) \end{bmatrix} \text{.....(2)}$$

It can be observed from (2) that ud includes the amplitude information of the input signal while uq includes the phase error information. By using the PI regulator as the LF to control uq to zero and sending it to the VCO (represented by an integrator), the estimated phase angle θPLL can be equal to that of the input [14]. According to the Mason formula, the transfer functions from ug to uα and uβ can be deduced as

$$G\alpha(s) = u\alpha(s) / ug(s) = ke\omega PLLs / (s\,2 + ke\omega PLLs + \omega\,2\,PLL) \quad \text{..... (3)}$$

$$G\beta(s) = u\beta(s) / ug(s) = ke\omega\,2\,PLL\,s\,2 + ke\omega PLLs + \omega\,2\,PLL \quad \text{..... (4)}$$

where, in the steady state, ωPLL is 2π50 rad/s.

IV. SIMULATION AND RESULTS

In this section simulation model of the wind energy conversion system (which operates in both standalone and grid connected modes) is studied. Five different cases will also be studied by varying the wind speed and load. In the first case wind speed remains constant and the output powers i.e. wind power, battery power, power at PCC, load power and grid power are observed and their balance is also observed. In the remaining cases, a step signal is used at the place of wind speed to represent varying wind speed and then the power balance is observed at various loads.

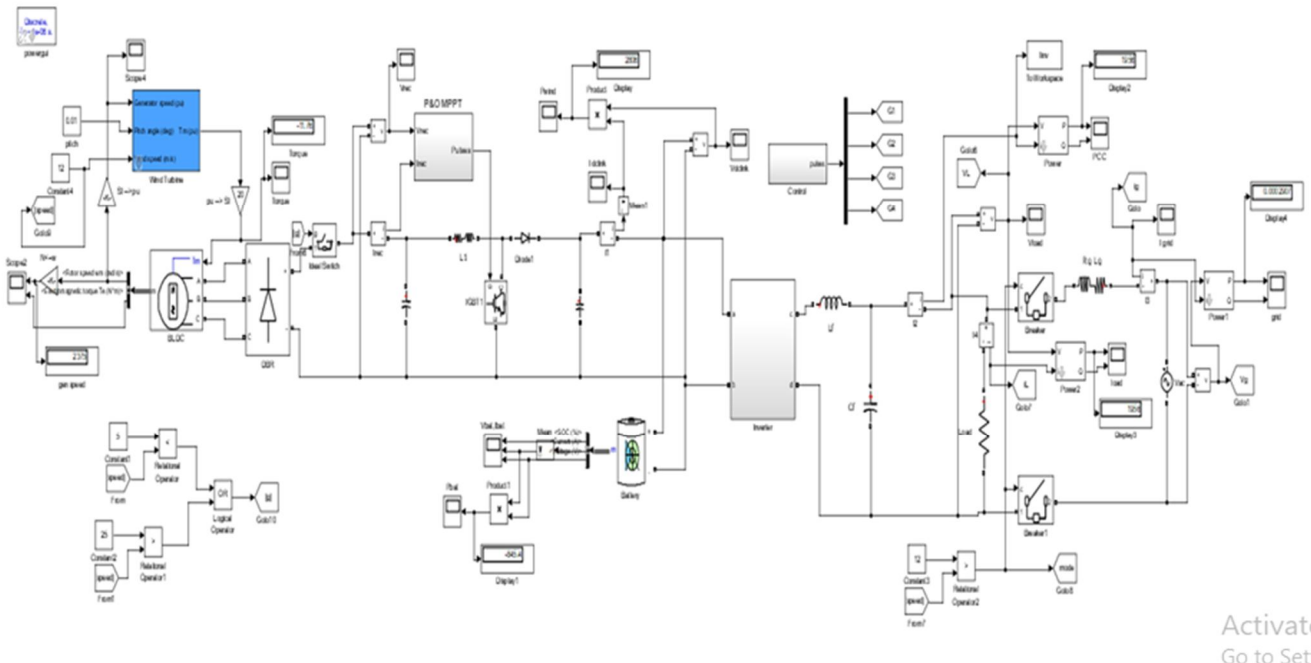


Fig. 7. Simulink model of the microgrid

1) *Case(i):* Wind power and Grid supply the load, Battery charging in this case, wind speed vw=12 m/s, Load= 5000W

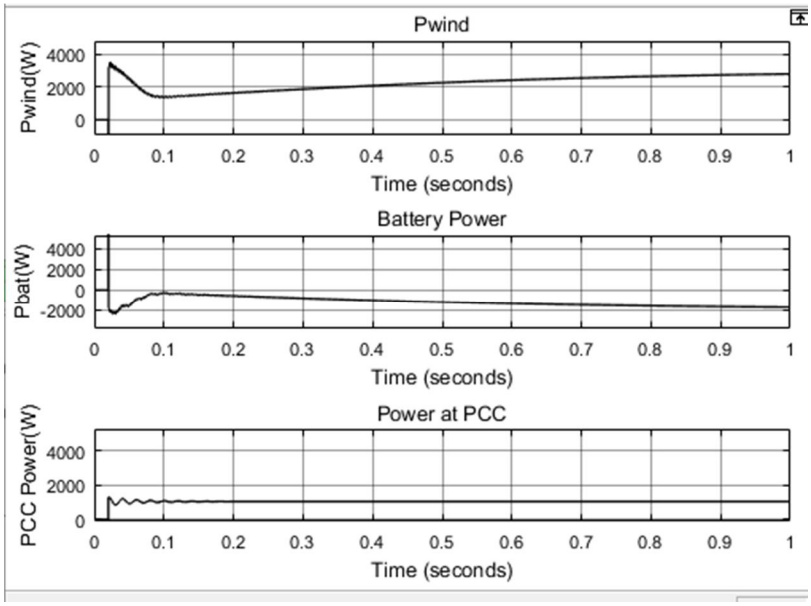


Fig. 8. Wind power, Battery power and Power at PCC

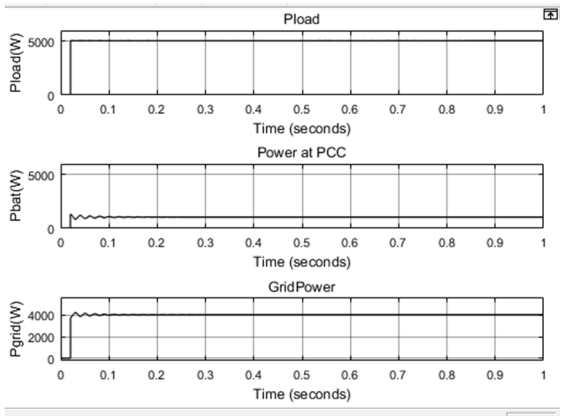


Fig. 9. Powers at Load, PCC and Grid

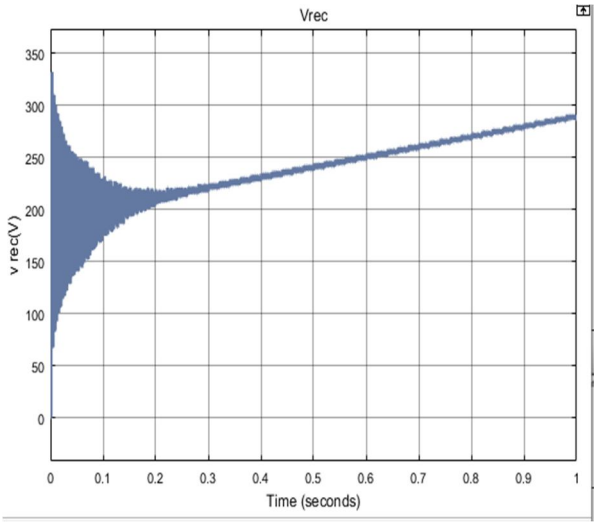


Fig. 10. Output Voltage of the rectifier

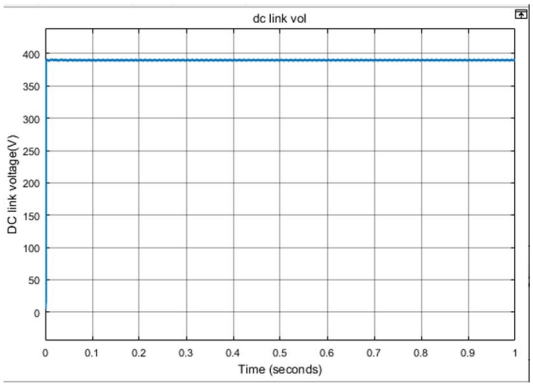


Fig. 11. Voltage at DC link

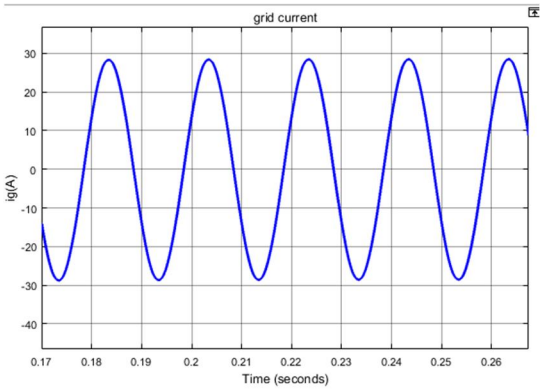


Fig. 12. Grid current

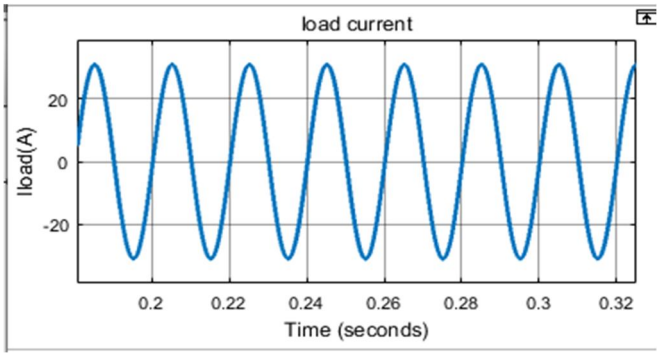


Fig. 13. Load current

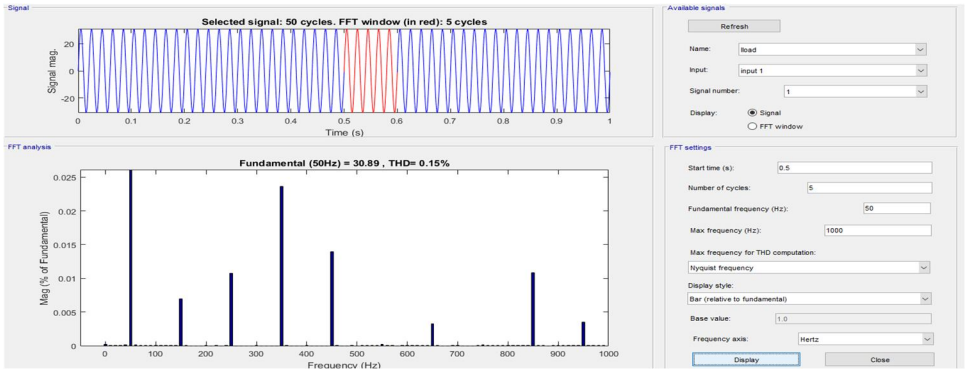


Fig. 14. FFT analysis of load current (THD=0.15%)

Table II: Observations for load=5000W, wind speed=12m/s

P_{wind}	2805W
$P_{battery}$	-1748W (Charging)
P(PCC)	1022W
P_{load}	5025W
P_{grid}	4043
Torque	11.746 Nm
N_{gen}	2376rpm

2) *Case(ii):* Desynchronisation-Wind speed changes from 10 m/s to 13 m/s, Load= 5000W: In this initially when the wind speed is 10m/s the microgrid operates in grid connected mode and at t=0.5 when speed changes to 13m/s from 10m/s the microgrid switches to standalone mode.

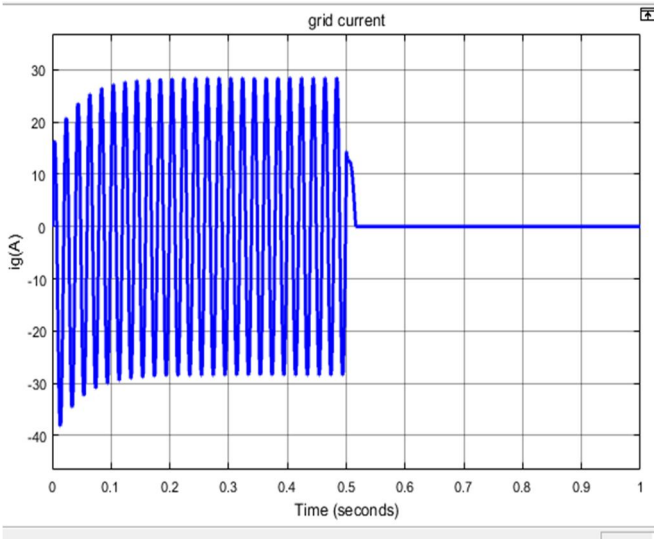


Fig. 15. Grid Current

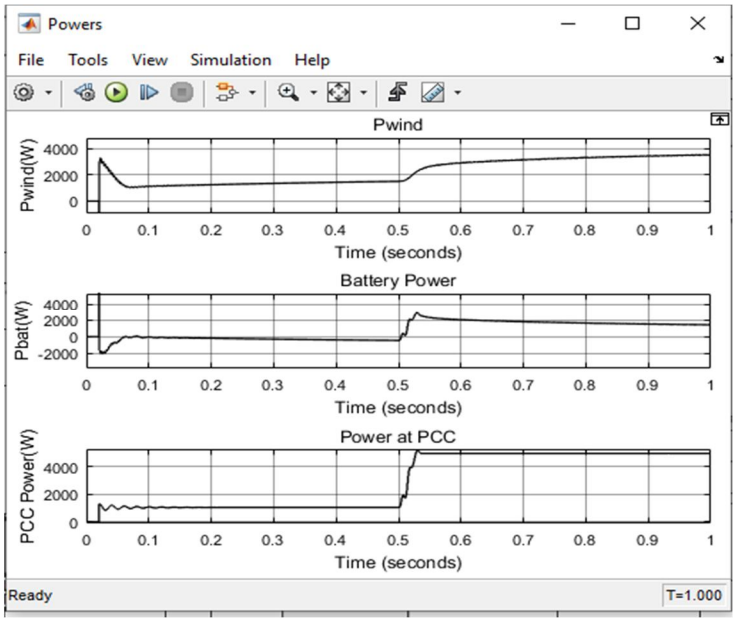


Fig. 1. Wind Power, Battery Power and Power at PCC

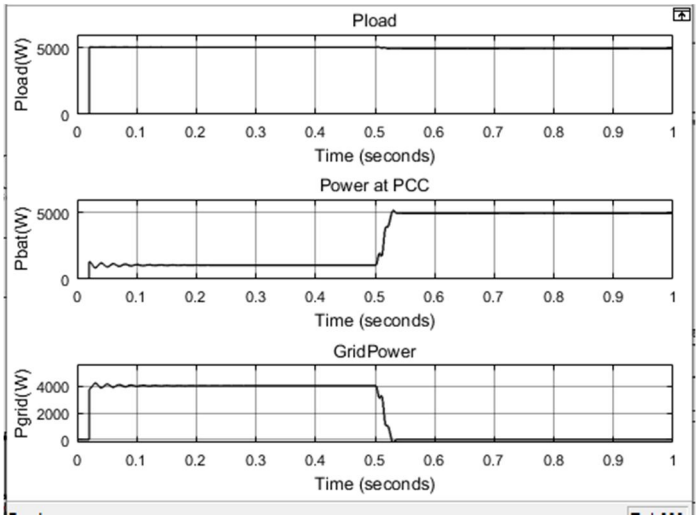


Fig. 2. Load Power, power at PCC and Grid Power

TABLE III: OBSERVATIONS WHEN LOAD=5KW, WHEN WIND SPEED CHANGES FROM 10M/S TO 13M/S

	At t=0.5s	At t=1s
P_{wind}	1500 W	3538 W
$P_{battery}$	-500 W (charging)	1432 W(discharging)
$P_{(PCC)}$	1000 W	4955 W
P_{load}	5000 W	4955W
P_{Grid}	4000 W	0W
Torque	11.685 Nm	13.69 Nm
Gen speed(N)	2050 rpm	2528rpm

3) Case(iii): Synchronisation, Load=3.5KW

In this case load is considered to be 3.5KW, let the wind speed change from 12.5m/s to 10.8 m/s i.e. the synchronization of micro grid takes place. The wave forms for grid current, Power developed by the wind, Battery power, Power at PCC, Load Power and Grid Power are shown. An observation table (i.e. Table III) is also provided which shows the magnitudes of powers at t=0.5s and t=1s.

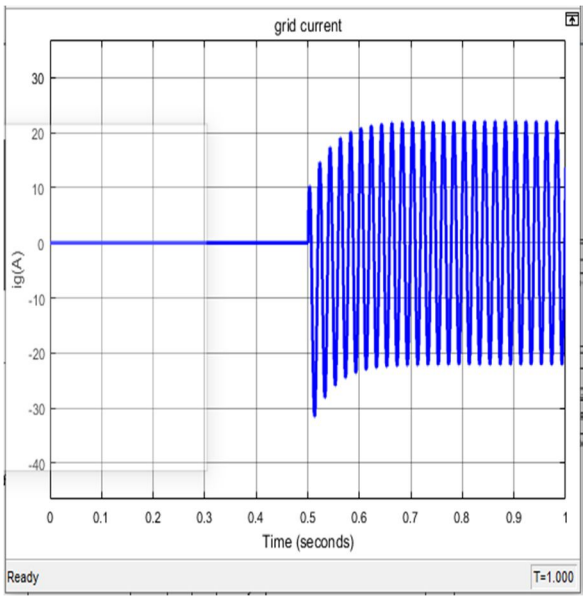


Figure3. Grid Current

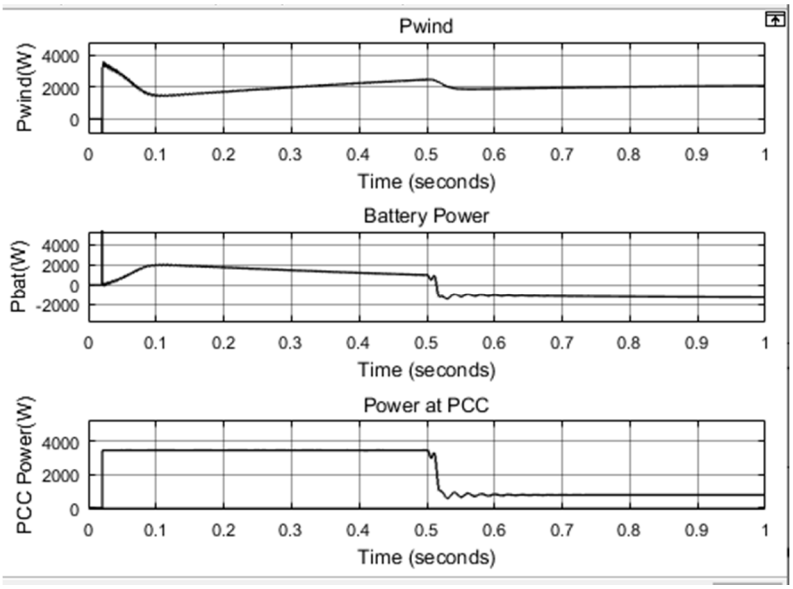


Figure 4. Wind Power, Battery Power and Power at PCC

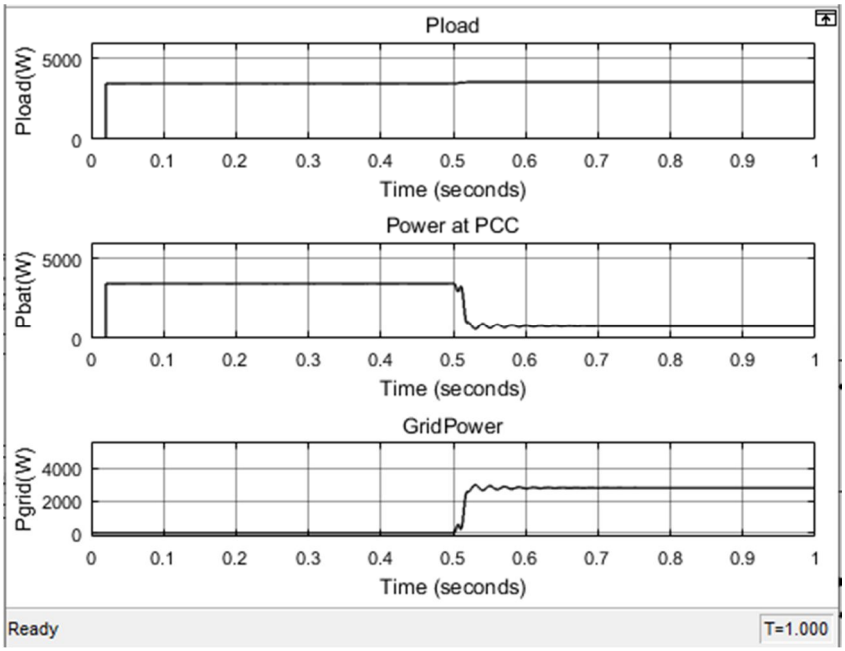


Figure 5. Load Power, Power at PCC, Grid Power

TABLE IIIII: OBSERVATIONS WHEN WIND SPEED CHANGES FROM 12.5M/S TO 10.8 M/S, LOAD=3500W

	At t=0.5s	At t=1s
P_{wind}	2470 W	3538 W
$P_{battery}$	990 W (discharging)	-1298 W(charging)
$P_{(PCC)}$	3445 W	783 W
P_{load}	3552 W	3552W
P_{Grid}	0 W	2798 W
Torque	11.04 Nm	9.266 Nm
Gen speed(N)	2050 rpm	2250 rpm

4) Case (iv): Desynchronisation, load=4000W

In this case, the load is considered to be 4000W and the speed of the wind changes from 11m/s to 12.8m/s at t=0.5s i.e the microgrid desynchronizes from the main grid.

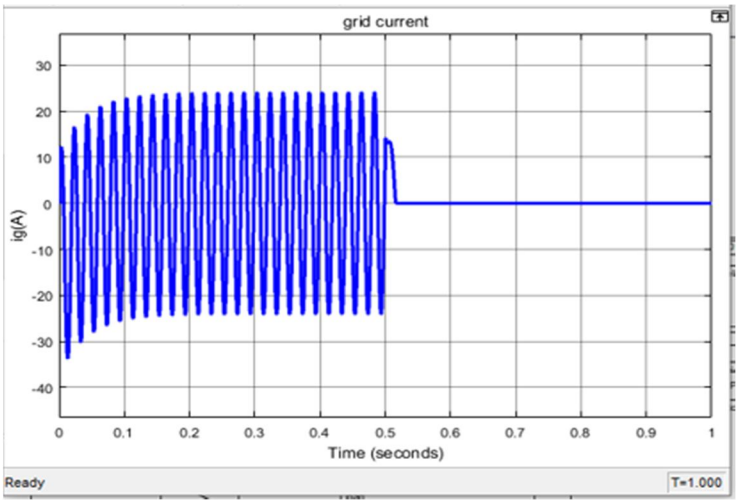


Figure 6. Grid Current

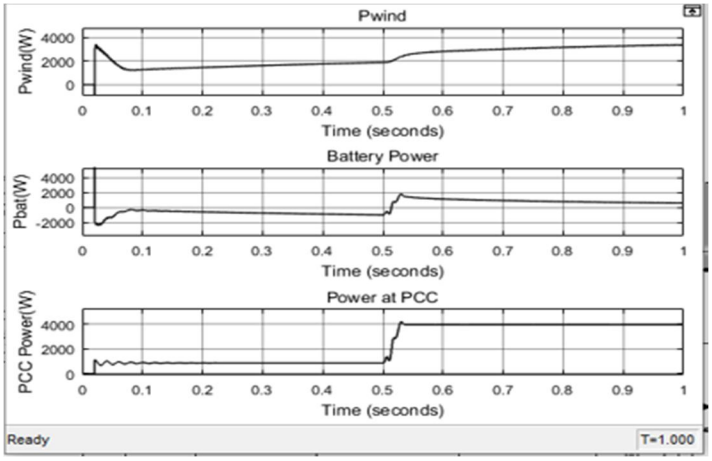


Figure 7. Wind Power, Battery Power, Power at PCC

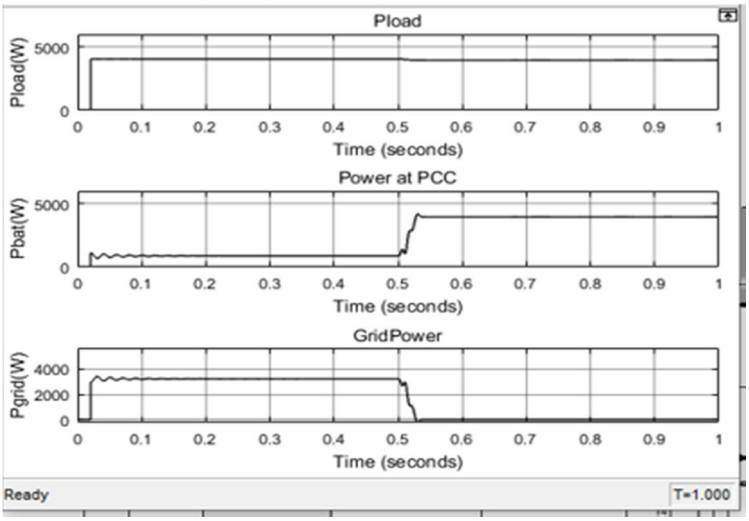


Fig. 8. Load Power, Power at PCC, Grid Power

TABLE IVV: OBSERVATIONS FOR LOAD =4KW, WHEN WIND SPEED CHANGES FROM 11M/S TO 12.8M/S

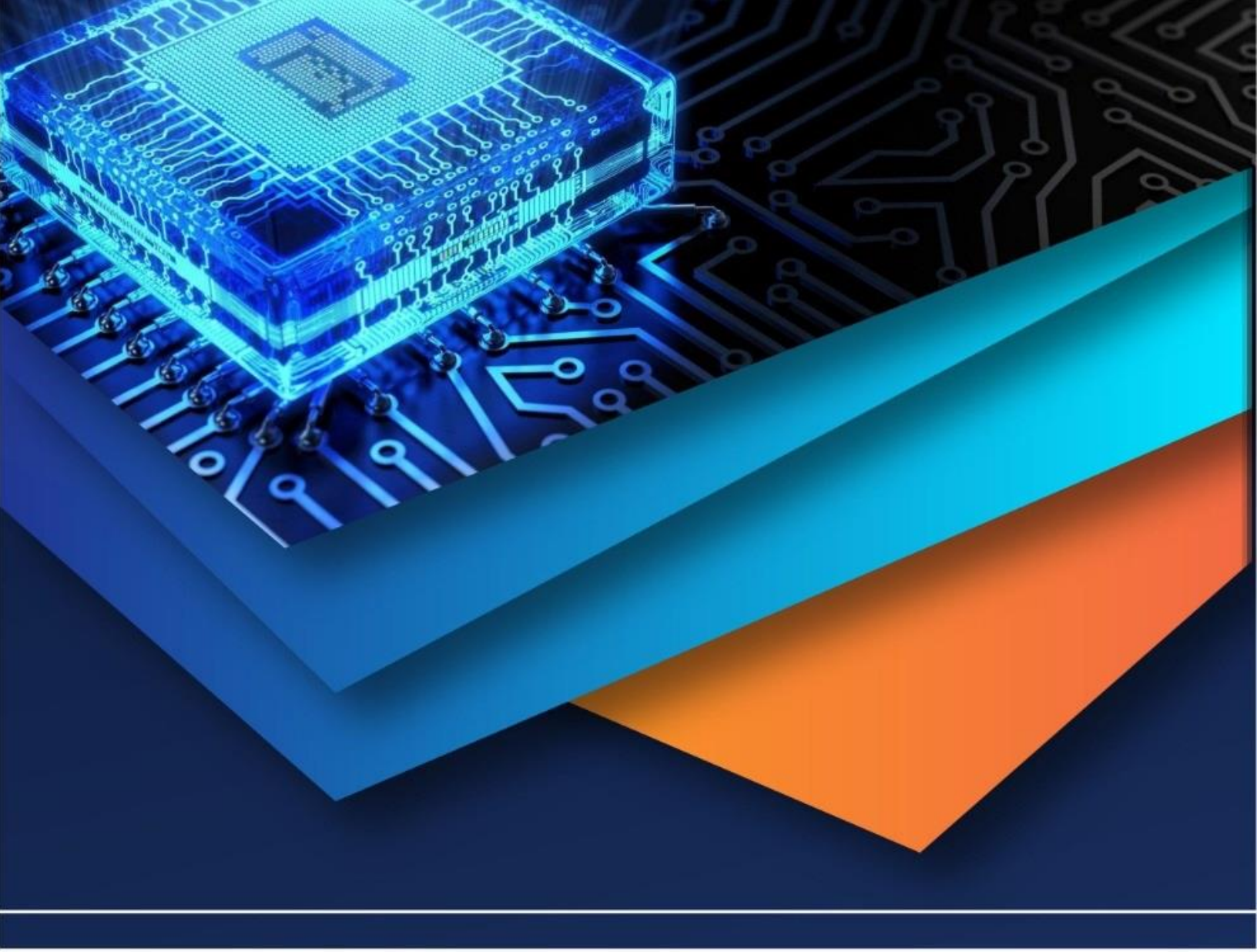
	At t=0.5s	At t=1s
P_{wind}	1980 W	3375 W
$P_{battery}$	-1000 W (charging)	592 W(discharging)
$P_{(PCC)}$	880 W	3956 W
P_{load}	3956 W	3956W
P_{Grid}	3100 W	0 W
Torque	11.2 Nm	13.47 Nm
Gen speed(N)	1900 rpm	2488 rpm

V. CONCLUSIONS

A wind based microgrid has been modelled and its performance is simulated in MATLAB/Simulink. The microgrid has worked in standalone environment with the wind availability. When the wind speed decreases the microgrid synchronises with the utility grid i.e. the control transfers from voltage control to current control. MPPT (Perturb and Observe) has been used to extract maximum power. The synchronization and de-synchronization processes are achieved seamlessly. During both the modes of operation (standalone and grid connected), the system steady state responses are observed satisfactorily for varying wind speeds and loads.

REFERENCES

[1] Geetha Pathak, Bhim Singh and B. K. Panigrahi, “Grid Synchronisation of Wind Based Microgrid”, 1st IEEE International Conference on Power Electronics, Intelligence Control and Energy Sytems(ICPEICES) 2016
[2] Ryan Mulholland, Victoria McBride, Catherine Vial, Adam O'Malley, and Drew Bennett, "2015 Top Markets Report Renewable Energy", July 2015. (www.trade.govlindustry)
[3] Mehmet Bilgili, Arif Ozbek, Besir Sahin, and Ali Kahraman, "A overview of renewable electric power capacity and progress in new technologies in the world." Renewable and Sustainable Energy Reviews on ELSEVIER, vol. 49, 323-334, sept. 2015.
[4] O. Khan and W. Xiao, "An Effiicient Modeling Technique to Simulate and Control Submodule-Integrated PV System for Single¬ Phase Grid Connection," IEEE Transactions on Sustainable Energy, vol. 7, no. 1, pp. 96-107, Jan. 2016.
[5] P. Hou, W. Hu, B. Zhang, M. Soltani, C. Chen and Z. Chen, "Optimised power dispatch strategy for offshore wind firms," lET on Renewable Power Generation, vol. 10, no. 3, pp. 399-409, 3 2016.
[6] R. Karki, P. Hu and R. Billinton, "Reliability Evaluation Considering Wind and Hydro Power Coordination," in IEEE Trnsactions on Power Systems, vol. 25, no. 2, pp. 685-693, May 2010.
[7] R. Lasseter, A. Akhil, C. Marnay, J. Stephens, J. Dagle, R. Guttromson, et al., "The CERTS microgrid concept," White paper for Transmission Reliabilit Program, Office of Power Technologies, US Department of Energ, 2002.
[8] U. K. Kalla, B. Singh and S. S. Murthy, "Modified electronic load controller for constant frequency operation with voltage regulation of small hydro driven single-phase SEIG," IEEE Industry Applications Society Annual Meeting, Addison, TX, 2015, pp. 1-8.
[9] B. Singh and R. Niwas, "Power Quality Improvement of PMSG ¬Based DG Set Feeding Three-Phase Loads," IEEE Transactions on Industry Applications, vol. 52, no. I, pp. 466-471, Jan.-Feb. 2016
[10] S.S. Thale, R.G. Wandhare and V. Agarwal, "A Novel Reconfigurable Microgrid Architecture With Renewable Energy Sources and Storage," IEEE Transactions on Industry Applications, vol. 51, no. 2, pp. 1805-1816, March-April 2015.
[11] M. Badoni, A. Singh and B. Singh, "Comparative Performance of Wiener Filter and Adaptive Least Mean Square-Based Control for Power Quality Improvement," IEEE Transactions on Industrial Electronics, vol. 63, no. 5, pp. 3028-3037, May 2016.
[12] C. Jain and B. Singh, "A Three-Phase Grid Tied SPV System With Adaptive DC Link Voltage for CPI Voltage Variations," IEEE Transactions on Sustainable Energy, vol. 7, no. 1, pp. 337-344, Jan. 2016.
[13] D. Dong, Timothy Thacker, Igor Cvetkovic, Rolando Burgos, Dushan Boroyevich, Fred Wang, and Glenn Skutt, "Modes of Operation and System-Level Control of Single-Phase Bidirectional PWM Converter for Microgrid Systems," IEEE Transactions on Smart Grid, vol. 3, no. 1, pp. 93-104, March 2012.
[14] H. Kim, T. Yu and S. Choi, "Indirect Current Control Algorithm for Utility Interactive Inverters in Distributed Generation Systems," IEEE Transactions on Power Electronics, vol. 23, no. 3, pp. 1342-1347, May 2008.



10.22214/IJRASET

45.98

IMPACT FACTOR: 7.129

IMPACT FACTOR: 7.429

INTERNATIONAL JOURNAL FOR RESEARCH

IN APPLIED SCIENCE & ENGINEERING TECHNOLOGY

Call : 08813907089 (24*7 Support on Whatsapp)